E C I 2 2 7 3 B
Journal Name Manuscript No.
Dispatch: 18.2.10 Journal: ECI CE: Ponjesuraj
Author Received: No. of pages: 8 PE: Gomathi
DOI: 10.1111/j.1365-2362.2010.02273.x

ORIGINAL ARTICLE

Altered membrane glycoprotein targeting in cholestatic hepatocytes

Giuseppa Esterina Liquori*, Maria Mastrodonato*, Roberta Rossi*, Giovanni Scillitani*, Patrizia Gena*, Piero Portincasa†, Giuseppe Calamita* and Domenico Ferri*

*University of Bari, Bari, Italy, †University of Bari Medical School, Bari, Italy

ABSTRACT

Background Hepatocytes are polarized epithelial cells with three morphologically and functionally distinct membrane surfaces: the sinusoidal, lateral and canalicular surface domains. These domains differ from each other in the expression of integral proteins, which concur to their polarized functions. We hypothesize that the cholestasis-induced alterations led to partial loss of hepatocyte polarity. An altered expression of membrane proteins may be indicative of functional disorders. Alkaline liver phosphatase (ALP), one of the most representative plasma membrane glycoproteins in hepatocytes, is expressed at the apical (canalicular) pole of the cell. Because the release of ALP protein in the bloodstream is significantly increased in cholestasis, the enzymatic levels of plasma ALP have major relevance in the diagnosis of cholestatic diseases. Here we assess the cholestasis-induced redistribution of membrane glycoproteins to investigate the ALP release.

Materials and methods We performed enzymatic histochemistry, immunohistochemistry, lectin histochemistry, immunogold and lectin-and immunoblotting studies. Experimental cholestasis was induced in rats by ligation of common bile duct (BDL).

Results The BDL led to altered membrane sialoglycoprotein targeting as well as to ultrastructural and functional disorders. Disarrangement of the microtubular system, thickening of the microfilamentous pericanalicular ectoplasm and disturbance of the vectorial trafficking of membrane glycoprotein containing vesicles were found.

Conclusions Altogether, results indicate that the cholestasis-induced partial loss of hepatocyte cell polarity leads to mistranslocation of ALP to the sinusoidal plasma membrane from where the enzyme is then massively released into the bloodstream.

Keywords Alkaline liver phosphatase, cholestasis, lectin histochemistry, membrane glycoproteins, ultrastructure.

Eur J Clin Invest 2010

Introduction

The hepatocyte plasma membrane has three morphologically and functionally distinct domains: (i) the apical (canalicular) membrane, formed by the invagination of two adjacent membranes and delimited by tight junctions, (ii) the lateral membrane, characterized by gap and desmosomal junctions and (iii) the sinusoidal membrane, characterized by microvilli projecting into Disse's space. These morphological domains differ from each other mainly in the expression of integral proteins, which concur to the polarized functions of the plasma membrane. Many of these proteins are glycosylated, such as the alkaline liver phosphatase (ALP) at the apical pole of hepatocytes and cholangiocytes from which it is secreted into bile in large amounts [1]. ALP is an *N*-glycosylated protein consisting of two equal subunits hydrolysing phosphate compounds such as phospholipids that are excreted into the bile canalicular lumen [2]. ALP has been suggested to play an active role in down-regulating the secretory activities of the intrahepatic biliary epithelium [1]. The sinusoidal plasma membrane is of pivotal importance in the movement of water and solutes between portal blood and hepatocyte interior and a site of hormone receptors and growth factors. Alterations in the expression of hepatocytes membrane proteins may indicate disorders of the liver function. Consistent with this idea, the strong increase in plasma ALP characterizing the cholestatic diseases [3,4] is associated with alterations in the distribution of ALP in the lateral and sinusoidal domains of hepatocyte

plasma membrane [5]. However, the mechanism underlying the release of ALP into the bloodstream remains poorly understood. It has been hypothesized [5] that the neo-synthesized ALP is translocated to the canalicular membrane and moves from there to the lateral domain through impaired tight junctions, before reaching the sinusoidal membrane and being released into the bloodstream [5]. Nevertheless, alternative pathways may also exist as suggested by the fact that the cholestatic hepatocyte undergoes ultrastructural alterations that affect the intracytoplasmic vesicular trafficking towards the canalicular membrane [6]. Here, we use rats with bile duct ligation, a validated animal model of obstructive cholestasis, to address the cholestasis-induced redistribution of hepatocyte sialylated membrane glycoproteins by having a close look at the release of ALP.

Materials and methods

Animals and treatment

Adult male Wistar rats (250–300 g; Harlan, Italy) were maintained on a standard diet and water *ad libitum*, and housed in a temperature- and humidity-controlled environment under a constant 12-h light-dark cycle. Under ether anaesthesia, the common bile duct was double-ligated and cut between the ligatures. Control animals underwent a sham operation that consisted of exposure, but not ligation, of the common bile duct. After 7 days of ligation, the animals were sacrificed and livers were harvested for evaluation. Each experimental (BDL) or control (sham-operated rats) group consisted of three to five rats. Deregulated bile flow was verified by assaying the serum alkaline phosphatase activity and total bilirubin level after 1, 3 and 7 days of surgery as previously described [7]. The protocol was conducted according to the Guide Principles for the care and use of laboratory animals.

Light microscopy

Both BDL and sham-operated rat specimens for light microscopy were fixed in 10% formalin, dehydrated in a series of graded ethanol and embedded in paraffin wax. Serial sections, 5-μm thick, were then cut.

Lectin histochemistry. Binding with two lectins, wheat germ agglutinin (WGA) and succinyl wheat germ agglutinin (S-WGA), was performed with the procedures previously described [8] to determine the distribution of *N*-acetylglucosaminyl and sialic acid residues on the membrane domains. WGA lectin has a binding specificity for sialic acid and *N*-acetyl-glucosamine, whereas S-WGA binds to $[\beta\text{-}(1\text{-}4)\text{-D-GlcNAc}]_2$ dimers [9]. WGA-FITC, S-WGA-FITC conjugated lectin and WGA-peroxidase conjugated were supplied by EY Laboratories, San Mateo, CA, USA.

Enzymatic histochemistry. To detect endogenous alkaline phosphatase activity, rehydrated sections were incubated in 0·2% Tween-20/PBS for 10 min and then rinsed in PBS for 10 min. Solubilization of membranes with non-ionic detergent increased detectable alkaline phosphatase activity [10]. The sections were incubated for 2 h at RT in substrate working solution in TBS pH 9·5 (BCIP/NBT Alkaline Phosphatase substrate Kit IV; Vector Laboratories). Reactions 2
were performed in the dark. The sections were washed in TBS pH 9·5 for 5 min, counterstained with fast-red, dehydrated, cleared and mounted with Neo-Entellan (Merck, Darmstadt, Germany).

Immunohistochemistry. For immunohistochemical assay, sections were incubated with the primary rabbit antibody against the ALP (Abcam, Cambridge, MA, USA) diluted 1 : 50 in blocking buffer at 4 °C. Analyses were performed as previously described [11].

Electron microscopy

For electron microscopy, BDL and sham-operated rat liver specimens were fixed and embedded in Epon-Araldite (Taab, Reading, UK) as previously described [11].

Immunoelectron microscopy. For immunoelectron microscopy, ultra-thin, non-osmicated sections were mounted on formwar-coated gold grids and incubated overnight with WGA 3
lectin conjugate with colloidal gold (15-nm diameter) diluted 1 : 200 in distilled water. Other sections were incubated overnight with the primary rabbit antibody against ALP (Abcam) diluted 1 : 50 in blocking buffer at 4 °C. Analyses were performed as previously described [11]. The grids were observed under a Morgagni 268 electron microscope (FEI, Hillsboro, OR, USA).

Preparation of liver microsomal membrane fraction. Livers from both BDL and sham-operated rats were quickly removed and homogenized with a Potter-Elvejem homogenizer (4 strokes in 1 min at 500 rpm) in an isolation medium 4
consisting of 220 mM mannitol, 70 mM sucrose, 20 mM Tris–HCl, 1 mM EDTA and 5 mM EGTA, pH 7·4 added of a cocktail of inhibitors (1 mM PMSF, 1 mM leupeptin, 1 mM pepstatin A). The homogenate was centrifuged at 500 *g* for 10 min at 4 °C and the pellet consisting of nuclei and unbroken cells was discarded; the resulting supernatant was centrifuged at 20 000 *g* for 20 min at 4 °C and the pellet consisting of mitochondria and plasma membrane-enriched fractions was discarded. For the isolation of the microsomal membrane-enriched fraction, the 20 000 *g* supernatant was centrifuged at 200 000 *g* for 1 h at 4 °C and the related pellet was collected and used for the immuno- or lectin

blotting. All chemicals used for the preparation were from Sigma.

Immuno- and lectin blotting. Aliquots (30 μg of proteins) of microsomal membrane fractions prepared as above were heated to 37 °C for 30 min and electrophoresed in an SDS/10% acrylamide gel using a high molecular weight protein ladder (Invitrogen, Carlsbad, CA, USA). The resolved proteins were transferred electrophoretically onto PVDF membranes that were blocked in 5% (w/v) low fat milk in blocking buffer (20 mM Tris–HCl, 0·15 M NaCl, 1% Triton-X-100, pH 7·5) for 1 h, and further incubated overnight at 4 °C with affinity purified rabbit polyclonal antibodies against anti-alkaline phosphatase (Abcam, Cambridge, UK) or WGA-peroxidase conjugated lectin (EY Laboratories) at a final concentration of 2 and 50 μg mL^{-1} in blocking solution, respectively. Horseradish peroxidase antirabbit IgG treated membranes (anti-rabbit IgG peroxidase antibody, Sigma) and WGA-peroxidase conjugated lectin blots were developed by luminol-chemiluminescence as previously reported [12,13].

Results

Light microscopy

Control rat liver. In sham-operated rat livers, most hepatocytes showed strong WGA binding over bile canalicular membrane whereas the reaction was reduced on basolateral domains (Fig. 1a,b). Moderate affinity for succinyl-WGA was only seen on canalicular membrane. Only a few canaliculi, mainly in periportal areas, showed alkaline phosphatase (ALP) activity, whereas basolateral membrane appeared unreactive (Fig. 1c). ALP activity was not seen in control sections preincubated with levamisolo (data not shown). Immunolabelling with anti-ALP was seen as scattered spots mainly in the cytoplasm (Fig. 1d).

Cholestatic rat liver. WGA binding of the canalicular membrane was lower than that of the control counterpart. Diffuse WGA staining was seen in the subcanalicular cytoplasm (Fig. 1e–g). Overall, the ALP activity was not homogeneously expressed over the hepatic lobules. In some cholestatic hepatocytes, ALP membrane activity was seen over the bile canaliculus, a profile similar to that characterizing the sham counterpart, while others showed most ALP enzymatic activity in the subcanalicular cytoplasm. This pattern was comparable with that related to the WGA reactivity (Fig. 1h). Moreover, alkaline phosphatase activity appeared on the basolateral membrane. Enzymatic activity was not seen in control sections preincubated with levamisolo. The intracytoplasmic labelling of the cholestatic hepatocytes incubated with anti-ALP antibodies was particularly evident and appeared to be more accentuated than that of the sham counterpart (Fig. 1i).

Electron microscopy

Control rat liver. As expected [14,15], the livers of sham-operated rats showed morphological and functional heterogeneity in terms of hepatocytes within the hepatic acinus. The hepatocytes located in the periportal area differed from those in the pericentral area as a result of their different functional behaviours. Nevertheless, all hepatocytes showed a mitochondria-rich cytoplasm, lysosomes and nuclei that were often polyploid and a well-developed smooth endoplasmic reticulum (Fig. 2a). Glycogen stores were scattered among the vesicles of the smooth endoplasmic reticulum. Bile canaliculi appeared regular in shape with the related membrane forming abundant and elongated microvilli that protruded into the lumen of the canaliculus (Fig. 2a). Canaliculi were sealed by the tight junctions of adjacent hepatocytes. A thin pericanalicular ectoplasm, with a microfilamentous network, was found in the pericanalicular cytoplasm. The lateral domain had a smooth surface bearing several junction types. The basal domain, or sinusoidal membrane, had a microvillous surface. WGA-gold binding was mainly observed on microvilli of the canalicular membrane. Nevertheless, scattered gold particles were also seen over some intracytoplasmic vesicles and in the basolateral plasma membrane (Fig. 2b). With the anti-ALP gold conjugate, gold particles were only seen in some canalicular membrane and intracytoplasmic vesicles (Fig. 2c).

Cholestatic rat liver. Hepatocytes of cholestatic rat liver showed several ultrastructural alterations, mainly at the bile canaliculus level. Together with some canaliculi whose morphological profile was comparable to that seen with the control livers, a large number of cholestatic canaliculi was characterized by lacking microvilli and having a wide lumen (Fig. 2d). A certain number of transitional canalicular structures partly provided with microvilli and canaliculus-like membrane invaginations were also encountered. Cholestatic hepatocytes were also characterized by a widening of the pericanalicular ectoplasm, which sometimes appeared to be swollen and oedematous. WGA-gold binding was mainly observed in intracytoplasmic vesicles located in the subcanalicular cytoplasm (Fig. 2e) and basolateral membrane. Canalicular binding was lower than that in the sham-operated rat hepatocytes. With the anti-ALP antibody, gold particles were mainly seen in Golgi complex and intracytoplasmic vesicles (Fig. 2f,g). Immunolabelling of the canalicular membrane depended on canalicular type. Membrane of typical cholestatic canaliculi did not bind the ALP antibody.

LOW RESOLUTION COLOUR FIG

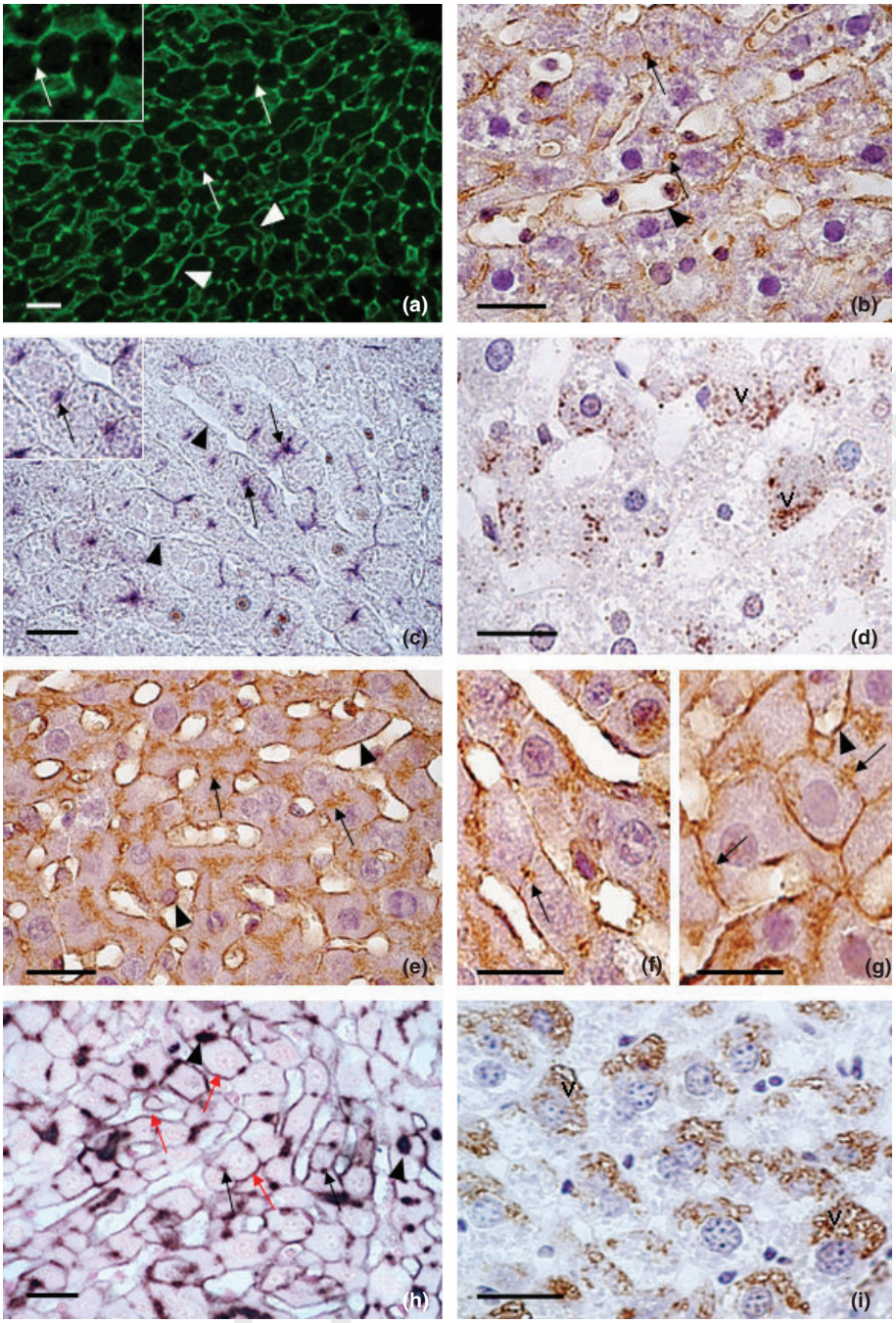

Figure 1 Histochemical features of normal (a,b,c,d) and cholestatic (e,f,g,h,i) rat liver hepatocytes. (a,b) In control rat liver, most hepatocytes show strong WGA binding on bile membrane (arrows); reaction is reduced on basolateral domains (*arrowheads*). a, WGA-FITC conjugated; b, WGA-peroxidase conjugated. (c) Only a few canaliculi, mainly in periportal areas, show alkaline phosphatase activity (arrows). Basolateral membrane (*arrowheads*) is unreactive. BCIP/NBT Alkaline Phosphatase substrate. (d) Immunolabelling with anti-ALP is seen, mainly in the cytoplasm as scattered spots (v). Anti-ALP peroxidase conjugated. (e) In cholestatic rat liver, WGA binding of the canalicular membrane is more than that of the control, whereas, generally, diffuse staining in the subcanalicular cytoplasm appears (arrows). Basolateral domains are reactive (*arrowheads*). WGA-peroxidase conjugated. (f) Some bile canaliculi show an evident membrane lectin-binding (arrow), as control WGA-peroxidase conjugated. (g) Most hepatocytes show diffuse staining in the subcanalicular cytoplasm (arrows) and evident staining of basolateral membranes (*arrowhead*). WGA-peroxidase conjugated. (h) Alkaline phosphatase activity is not homogeneously expressed within the hepatic lobule. In some hepatocytes, the bile canaliculus shows evident membrane enzyme activity, as in the control (black arrows), while in others the enzyme activity is strong and evident in the subcanalicular cytoplasm (*arrowheads*), the same as the WGA binding pattern, and moreover appeared on the basolateral membranes (red arrows). BCIP/NBT Alkaline Phosphatase substrate. (i) Intracytoplasmic labelling (v) with anti-ALP is more accentuated than the control. Anti-ALP peroxidase conjugated. Bars, 40 μm.

Lectin- and immuno-blotting

Immuno- and WGA-blotting experiments with microsomal membranes were performed to further analyse at a subcellular level the effect of BDL on the distribution of ALP and WGA-binding sites in liver.

Immunoblotting of sham rat liver microsomal membranes using rabbit anti-ALP polyclonal antibodies showed two reactive bands of molecular weights of about 57 and 110 kDa likely corresponding to the monomeric form of ALP and the related holoenzyme respectively (Fig. 3a). The same bands were seen

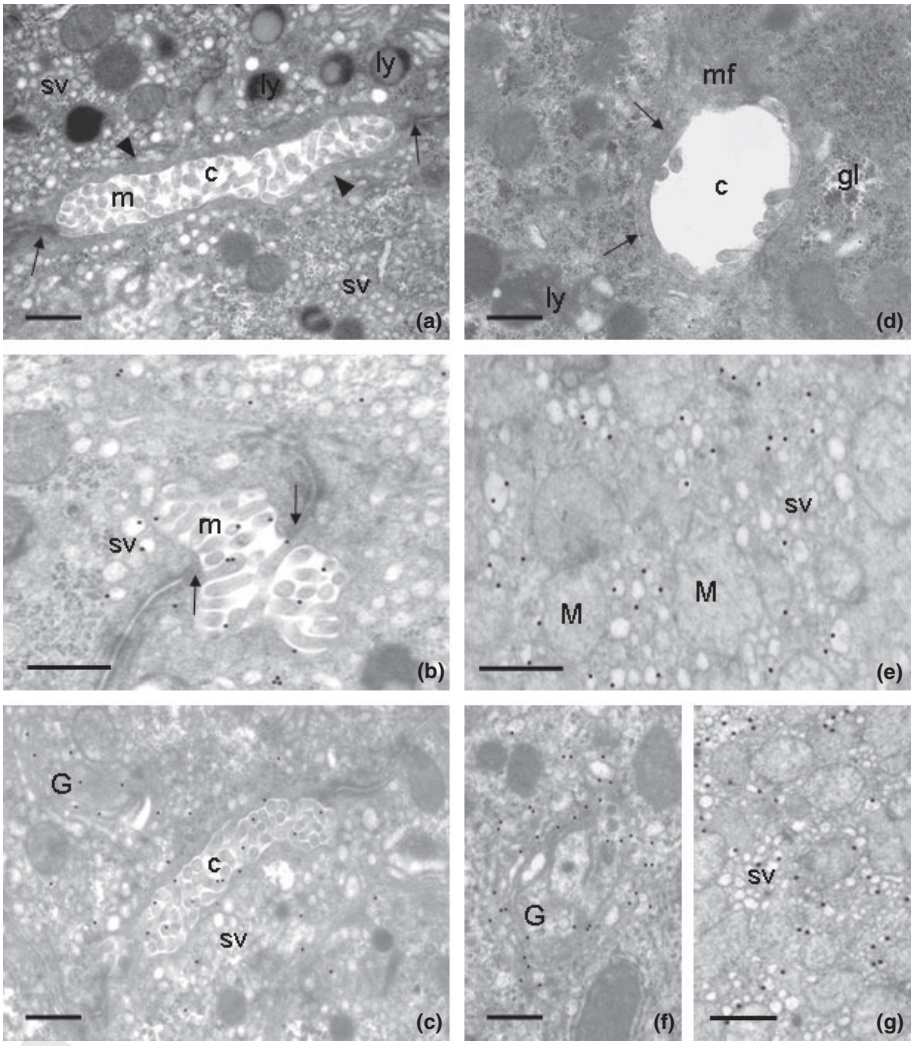

Figure 2 Ultrastructural and cytochemical features of normal (a,b,c) and cholestatic (d,e,f) rat liver hepatocytes. (a) In control rat liver, the bile canaliculi (c) are regular in shape, with abundant and elongated microvilli (m) protruding into the canalicular lumen, located between two adjacent hepatocytes and sealed by tight junctions (arrows). A thin ectoplasm with a microfilamentous network is evident in the pericanalicular cytoplasm (*arrowheads*). sv, smooth vesicles; ly, lysosomes. (b) WGA-gold binding is mainly observed on microvilli (m) of the canalicular membrane. However, scattered gold particles are also seen in the smooth vesicles (sv). arrows, tight junctions. (c) With the anti-ALP gold conjugate, scattered gold particles are seen in intracytoplasmic vesicles (sv) and in some canalicular membrane (c). G, Golgi complex. (d) Typical cholestatic hepatocytes show canaliculi (c) with a wide lumen devoid of microvilli. The pericanalicular ectoplasm (arrows) is wider than that of the control. Mf, microfilaments; gl, glycogen; ly, lysosome. (e) In cholestasis, WGA-gold binding is mainly observed on smooth vesicles (sv) located in the subcanalicular cytoplasm. Canalicular binding is more markedly reduced than that of the control rat liver. M, mitochondria. (f,g) With the anti-ALP gold conjugate, gold particles are mainly seen on the cysternae of the Golgi complex (G) and on intracytoplasmic vesicles (sv). Bars, 0·5 μm.

in the membranes from the BDL livers, although, consisting with the light and electron microscopy studies, their intensities were much higher (about 2·4-folds) than those detected in sham rat liver microsomes (Fig. 3b).

Multiple reactive bands were detected by lectin-blotting analysis using peroxidase-conjugated WGA (Fig. 3c). In line with the immunoblotting data, among these bands, two reactive bands of 57 and 110 kDa respectively, were found to be stronger (about 2·7-folds) in the BDL than in sham rat microsomal membranes (Fig. 3d). Additional sialylated glycoproteins were detected that were also found to be stronger in BDL than in sham conditions (Fig. 3c, *arrowheads*).

Discussion

The main finding in this study is that the expression and localization of WGA binding membrane glycoproteins is altered in the obstructive extrahepatic cholestasis induced by BDL as a consequence of a partial loss of hepatocyte polarity. Besides improving the knowledge of the morphological and functional alterations of cholestatic hepatocytes, this study provides valuable insights into the mechanism by which liver ALP is massively released into the bloodstream in cholestasis.

The results of enzymatic histochemistry show that in the hepatocytes of sham rats only a few canaliculi, mainly located in the periportal areas, have phosphatase activity. This pattern of enzymatic activity is not seen in the basolateral membrane by: (i) indicating that the profile of the WGA binding does not exactly correspond with the distribution of ALP and (ii) suggesting the presence of other sialylated glycoproteins other than ALP on the membrane of hepatocytes. This fully agrees with a previous study reporting the presence of multiple WGA-binding glycoproteins in the hepatocyte plasma membrane of healthy liver [16,17].

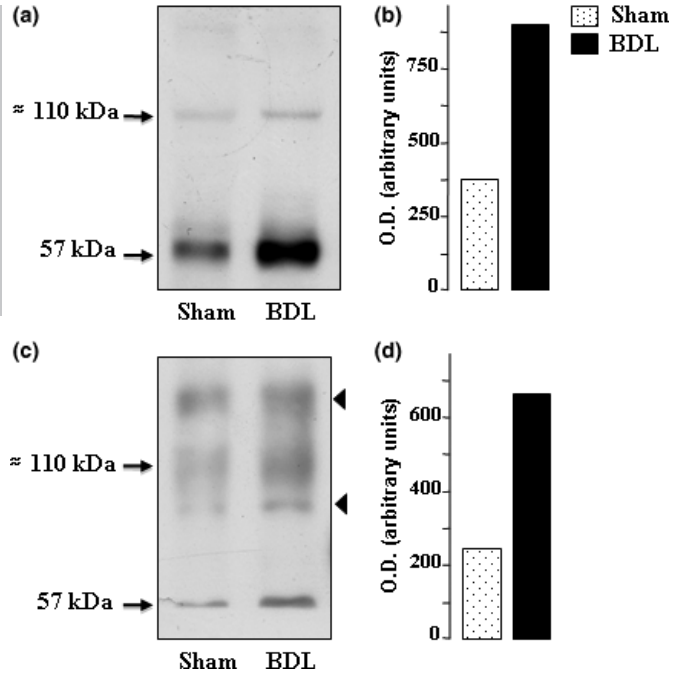

Figure 3 Immuno- and lectin-blotting analyses of liver microsomal membranes from sham-operated and BDL rats. (a) Immunoblotting with rabbit polyclonal anti-ALP antibodies. Two bands of 57 and 110 kDa (arrows), likely corresponding to the ALP monomer and the holoenzyme, respectively, are seen in both conditions. (b) Densitometric analysis. The overall intensity of the 57 and 110 kDa bands is stronger in the BDL than in sham condition. (c) Lectin-blotting using peroxidase-conjugated WGA. Bands of 57 and 110 kDa (arrows) are seen together with other sialylated glycoproteins (*arrowheads*). (d) Densitometric analysis. The overall intensity of the 57 and 110 kDa bands in the BDL condition is about 2·7 times higher than in the sham counterpart.

An interesting observation is the fact that the extent of the WGA binding glycoproteins in the canalicular membrane of cholestatic hepatocytes is significantly lower than that of the sham counterpart, whereas a diffuse staining is found in the pericanalicular cytoplasm. ALP activity is markedly increased in cholestasis and also appears on the lateral membrane and on the sinusoidal membrane, as previously observed [3–5].

Electron microscopy shows that in cholestatic hepatocytes, irregular dilation of the bile canaliculi lacking microvilli is accompanied by widening of the pericanalicular ectoplasm, hypertrophy of the smooth endoplasmic reticulum and severe alterations of the tight junctions and cytoskeleton [6,18,19]. Phosphatase activity has not been observed in cholestatic canaliculi [5,20]. In cholestatic hepatocytes, the fact that despite an increase in ALP on the basolateral membrane, a reduction in lectin reactivity on the membrane was still observed, may be ascribable to the loss of membrane (microvilli) rich in sialylated glycoproteins. An evident affinity for the WGA on the smooth vesicles in the pericanalicular cytoplasm was also observed. This profile may be attributable to an increase in phosphatase synthesis or an alteration of the cytoskeletal architecture and, consequently, vesicular trafficking. ALP is one of the few enzymes whose synthesis is increased in the liver in response to BDL [4,21–24]. Nevertheless, this is not enough to explain the consistent increase in intracytoplasmic ALP activity that may be also caused by obstruction of the translocation of glycoproteins to the apical plasma membrane.

Cholestasis causes an increase in microfilaments, with the consequent increase of ectoplasm, mainly pericanalicular [6], and probably alteration of the microtubular system. The structural alteration of the cytoskeleton could give rise to alteration of the intracellular trafficking of vesicles transporting ALP and other (glyco)proteins destined for the canalicular membrane. Anti-microtubular agents, such as cholchicine, interfere with the intracellular transport of plasma membrane proteins located in the apical domain of polarized epithelial cells [25,26]. The anomalous thick pericanalicular ectoplasm obstructs the trafficking of vesicles which accumulate in the subcanalicular cytoplasm and gives rise to the WGA binding and to the strong ALP expression, as indicated by the immunoblotting and lectin-blotting data. Alteration of the cytoskeleton may also be responsible for the increase in phosphatase expression on basolateral membrane and in blood plasma. It can be speculated that as a result of the alteration of the cytoskeleton, the ALP destined to the canalicular membrane reaches the basolateral membrane from which it is then released into the portal blood. Colchicine, which causes microtubule depolymerization, induces a redistribution of ALP towards the basolateral membrane as a result of an altered microtubule- dependent transport of vesicles [27–29]. Thus, it can be speculated that in cholestasis, the strong increase in serum ALP is resulting from the direct release of the enzyme from the sinusoidal membrane to the Disse's space and then to the blood plasma. This would exclude ALP release from the canalicular membrane to lateral membrane through impaired tight junctions, and subsequent release into the bloodstream by sinusoidal membrane [5]. Structural and functional alterations of tight junctions occurring during cholestasis [30] may also be involved in the redistribution of ALP and other membrane (glyco)proteins. In hepatocytes, the tight junctions separate bile canaliculi from the basolateral cell surface and represent a functional barrier between blood and bile. Hence, in line with a previous study [31], we hypothesize that impaired functional integrity of tight junctions following bile duct ligation underlies the partial loss of hepatocellular surface polarity.

Although the current experiment was designed to test the effect of short-term (7 days) obstructive cholestasis in rats, we can speculate that drug-induced liver injury associated with a cholestatic pattern also produce similar damage especially in the sub-chronic period. Typical cholestatic changes of drug-induced liver injury in the acute phase were missing in our histology (i.e. associated with hepatocellular or hepatocanalicular-cholangiolitic or inflammatory changes). Rather a picture of subchronic-chronic intrahepatic cholestasis (e.g. by amitriptyline, ampicillin, amoxicillin-clavulanate, carbamazepine, chlorpromazine, cyproheptadine, erythromycin and antidepressants etc.) might resemble the picture observed in this study [32]. Similarly, genetic defects inducing cholestasis in an early phase could resemble the picture in this study. Further studies should address these issues.

In conclusion, this work shows that common bile duct ligation induces ultrastructural and functional disorders similar to those caused by the anti-microtubular agent colchicine, with disarrangement of the microtubular system, thickening of the microfilamentous pericanalicular ectoplasm disturbance of the vectorial transport of membrane-glycoprotein containing vesicles and consequently, partial loss of polarity of the hepatocytes. This alteration of the cytoskeleton seems to be responsible for the direct redistribution of ALP to the sinusoidal membrane and consequent release into bloodstream.

Address

Department of Animal and Environmental Biology, University of Bari, Bari, Italy (G. E. Liquori, M. Mastrodonato, G. Scillitani, D. Ferri); Laboratory of Ultrastructural Pathology, Department of Pathological Anatomy, University of Bari, Bari, Italy (R. Rossi); Department of General and Environmental Physiology, University of Bari, Bari, Italy (P. Gena, G. Calamita); Department of Internal Medicine, University of Bari Medical School, Bari, Italy (P. Portincasa).
Correspondence to: Prof. Domenico Ferri, Laboratory of Histology and Comparative anatomy, Department of Animal and Environmental Biology, University of Bari, Via Orabona, 4 – I 70125, Bari, Italy. Tel./fax: +390805443348;
e-mail: d.ferri@biologia.uniba.it

Received 30 September 2009; accepted 22 January 2010

References

1 Alvaro D, Alpini G, Onori P, Perego L, Svegliata Baroni G, Franchitto A *et al*. Estrogens stimulate proliferation of intrahepatic biliary epithelium in rats. *Gastroenterology* 2000;**119**:1681–91.
2 Chida K, Taguchi M. Localization of alkaline phosphatase and proteins related to intercellular junctions in rat hepatoma cell line McA-RH 7777. *J Histochem Cytochem* 2004;**52**:979–83.
3 Elsafi ME, Holmberg JT, Hultberg B, Hägerstrand I, Isaksson A, Joelsson B *et al*. Alkaline phosphatase in cholestatic and cirrhotic rats. A biochemical and histochemical study. *Enzyme* 1989;**42**:145–51.
4 Frederiks WM, Van Noorden CJ, Aronson DC, Marx F, Bosch KS, Jonges GN *et al*. Quantitative changes in acid phosphatase, alkaline phosphatase and 5′-nucleotidase activity in rat liver after experimentally induced cholestasis. *Liver* 1990;**10**:158–66.
5 Kako M, Toda G, Torii M, Kimura H, Miyake K, Suzuki H *et al*. Electron microscopic studies on hepatic alkaline phosphatase in experimentally induced biliary obstruction of the rat. *Gastroenterol Jpn* 1980;**15**:600–5.
6 Chung KW, Han NI, Choi SW, Ahn BM, Yoon SK, Nam SW *et al*. Increased microfilaments in hepatocytes and biliary ductular cells in cholestatic liver diseases. *J Korean Med Sci* 2002;**17**:795–800.
7 Carreras FI, Gradilone SA, Mazzone A, García F, Huang BQ, Ochoa JE *et al*. Rat hepatocyte aquaporin-8 water channels are down-regulated in extrahepatic cholestasis. *Hepatology* 2003;**37**:1026–33.
8 Liquori GE, Mastrodonato M, Zizza S, Ferri D. Glycoconjugate histochemistry of the digestive tract of Triturus carnifex (Amphibia, Caudata). *J Mol Histol* 2007;**38**:191–9.
9 Goldstein IJ, Hayes CE. The lectins: carbohydrate binding proteins of plants and animals. *Adv Carbohydr Chem Biochem* 1978;**35**:127–340.
10 Ey PL, Ferber E. Calf thymus alkaline phosphatase. II. Interaction with detergents. *Biochim Biophys Acta* 1977;**480**:163–77.
11 Ferri D, Mazzone A, Liquori GE, Cassano G, Svelto M, Calamita G. Ontogeny, distribution, and possible functional implications of an unusual aquaporin, AQP8, in mouse liver. *Hepatology* 2003;**38**:947–57.
12 Calamita G, Mazzone A, Cho YS, Valenti G, Svelto M. Expression and localization of the aquaporin-8 water channel in rat testis. *Biol Reprod* 2001;**64**:1660–6.
13 Mastrodonato M, Calamita G, Rossi R, Scillitani G, Liquori GE, Ferri D. Expression of H^+,K^+-ATPase and glycopattern analysis in the gastric glands of *Rana esculenta*. *J Histochem Cytochem* 2009;**57**:215–25.
14 Sell S. Heterogeneity and plasticity of hepatocyte lineage cells. *Hepatology* 2001;**33**:738–50.
15 Ferri D, Moro L, Mastrodonato M, Capuano F, Marra E, Liquori GE *et al*. Ultrastructural zonal heterogeneity of hepatocytes and mitochondria within the hepatic acinus during liver regeneration after partial hepatectomy. *Biol Cell* 2004;**97**:277–8.
16 McMillan PN, Hixson DC, Hevey KA, Naik S, Jauregui HO. Hepatocyte cell surface polarity as demonstrated by lectin binding. *J Histochem Cytochem* 1988;**36**:1561–71.
17 Hixson DC, Allison JP, Chesner JE, Leger MJ, Ridge LL, Walborg EF Jr. Characterization of a family of glycoproteins associated with the bile canalicular membrane of normal hepatocytes but not expressed by two transplantable rat hepatocellular carcinomas. *Cancer Res* 1983;**43**:3874–84.
18 Oda M, Phillips MJ. Bile canalicular membrane pathology in cytochalasin B-induced cholestasis. *Lab Invest* 1977;**37**:350–6.
19 Elias E, Hrubant Z, Wade JB, Boyer JL. Phalloidin-induced cholestasis: a microfilament-mediated change in junctional complex permeability. *Proc Natl Acad Sci USA* 1980;**77**:2229–33.
20 De Vos R, De Wolf-Peeters C, Desmet V, Bianchi L, Rohr HP. Significance of liver canalicular changes after experimental bile duct ligation. *Exp Mol Pathol* 1975;**23**:12–34.
21 Kaplan MM, Righetti A. Induction of rat liver alkaline phosphatase: the mechanism of the serum elevation in bile duct obstruction. *J Clin Invest* 1970;**49**:508–16.

22 Hatoff DE, Hardison WGM. Induced synthesis of alkaline phosphatase by bile acids in rat liver cell culture. *Gastroenterology* 1979;**77**:1062.
23 De Broe ME, Borgers M, Wieme RJ. The separation and characterization of liver plasma membrane fragments circulating in the blood of patients with cholestasis. *Clin Chim Acta* 1975;**59**:369.
24 Kaplan MM. Serum alkaline phosphatase: another piece is added to the puzzle. *Hepatology* 1986;**6**:526.
25 Taguchi M, Chida K. Effects of colchicines on localization of alkaline phosphatase in McA-RH 7777 rat hepatoma cells. *Acta Histochem Cytochem* 2008;**41**:149–55.
26 Chida K, Tamamushi S, Yamamoto I. Enzyme cytochemical study of alkaline phosphatase in rat hepatocytes – change of location after colchicine administration or bile duct ligation. *Okajimas Folia Anat Jpn* 1995;**71**:371–9.
27 Araki N, Takashima Y, Makita T. Redistribution and fate of colchicine-induced alkaline phosphatase in rat hepatocytes: possible formation of autophagosomes whose membrane is derived from excess plasma membrane. *Histochem Cell Biol* 1995;**104**:257–65.
28 Kaplan MM. Induction of rat liver alkaline phosphatase bile duct by ligation *Yale. J Biol Med* 1979;**52**:69–75.
29 Kaplan MM, Ohkubo A, Quaroni EG, Sze-Tu D. Increased synthesis of rat liver alkaline phosphatase by bile duct ligation. *Hepatology* 1983;**3**:368–76.
30 Takakuwa Y, Kokai Y, Sasaki K, Chiba H, Tobioka H, Mori M *et al.* Bile canalicular barrier function and expression of tight-junctional molecules in rat hepatocytes during common bile duct ligation. *Cell Tissue Res* 2002;**307**:181–9.
31 Landmann L, Meier PJ, Bianchi L. Bile duct ligation-induced redistribution of canalicular antigen in rat hepatocyte plasma membrane demonstrated by immunogold quantitation. *Histochemistry* 1990;**94**:373–9.
32 Zimmerman HJ, Lewis JH. Drug-induced hepatotoxicity. *Gastroenterol Clin North Am* 1995;**24**:1027.

Author Query Form

Journal: ECI

Article: 2273

Dear Author,
During the copy-editing of your paper, the following queries arose. Please respond to these by marking up your proofs with the necessary changes/additions. Please write your answers on the query sheet if there is insufficient space on the page proofs. Please write clearly and follow the conventions shown on the attached corrections sheet. If returning the proof by fax do not write too close to the paper's edge. Please remember that illegible mark-ups may delay publication.

Many thanks for your assistance.

Query reference	Query	Remarks
Q1	**AUTHOR: Please check the title, author names, affiliations and source of funding carefully.**	
Q2	**AUTHOR: Please give address information for 'Vector Laboratories': town, state (if applicable), and country.**	
Q3	**AUTHOR: Please check the expression: 'formwar-coated gold grids'.**	
Q4	**AUTHOR: 500 rpm: please replace this with the correct g value.**	
Q5	**AUTHOR: Please give address information for 'Sigma': town, state (if applicable), and country.**	
Q6	**AUTHOR: Instead of 'seen' shall we use 'observed'? Please check throughout the article.**	
Q7	**AUTHOR: Together with..... wide lumen. The meaning of this sentence is not clear; please rewrite or confirm that the sentence is correct.**	
Q8	**AUTHOR: The same bands..... liver microsomes. This sentence has been reworded for clarity. Please check and confirm it is correct.**	
Q9	**AUTHOR: Figure 1 has been saved at a low resolution of 122 dpi. Please resupply at 600 dpi. Check required artwork specifications at http://authorservices.wiley.com/submit_illust.asp?site=1**	
Q10	**AUTHOR: Figure 2 has been saved at a low resolution of 130 dpi. Please resupply at 600 dpi. Check required artwork specifications at http://authorservices.wiley.com/submit_illust.asp?site=1**	
Q11	**AUTHOR: Figure 3 has been saved at a low resolution of 125 dpi. Please resupply at 600 dpi. Check required artwork specifications at http://authorservices.wiley.com/submit_illust.asp?site=1**	

USING E-ANNOTATION TOOLS FOR ELECTRONIC PROOF CORRECTION

Required Software

Adobe Acrobat Professional or Acrobat Reader (version 7.0 or above) is required to e-annotate PDFs. Acrobat 8 Reader is a free download: http://www.adobe.com/products/acrobat/readstep2.html

Once you have Acrobat Reader 8 on your PC and open the proof, you will see the Commenting Toolbar (if it does not appear automatically go to Tools>Commenting>Commenting Toolbar). The Commenting Toolbar looks like this:

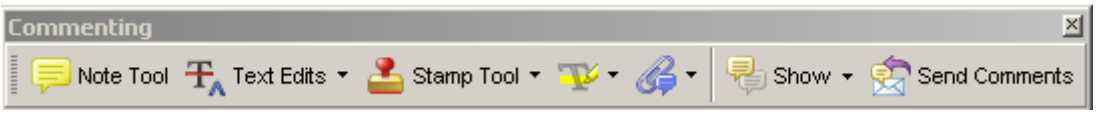

If you experience problems annotating files in Adobe Acrobat Reader 9 then you may need to change a preference setting in order to edit.

In the "Documents" category under "Edit – Preferences", please select the category 'Documents' and change the setting "PDF/A mode:" to "Never".

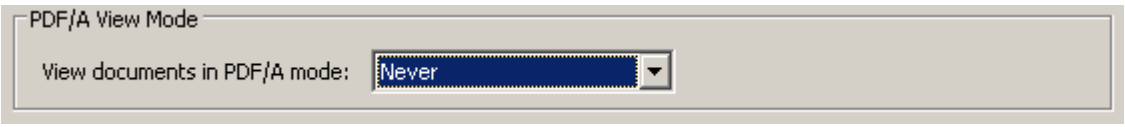

Note Tool — For making notes at specific points in the text

Marks a point on the paper where a note or question needs to be addressed.

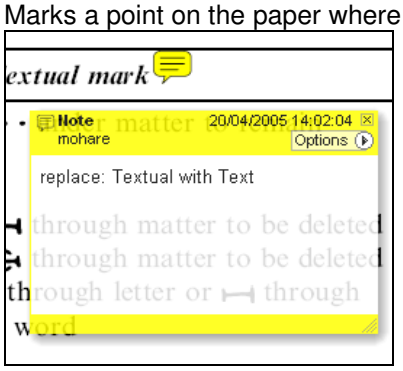

How to use it:

1. Right click into area of either inserted text or relevance to note
2. Select Add Note and a yellow speech bubble symbol and text box will appear
3. Type comment into the text box
4. Click the X in the top right hand corner of the note box to close.

Replacement text tool — For deleting one word/section of text and replacing it

Strikes red line through text and opens up a replacement text box.

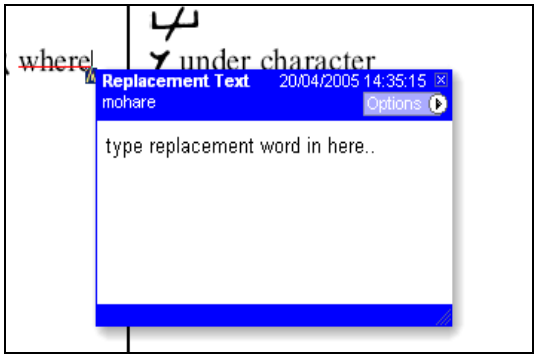

How to use it:

1. Select cursor from toolbar
2. Highlight word or sentence
3. Right click
4. Select Replace Text (Comment) option
5. Type replacement text in blue box
6. Click outside of the blue box to close

Cross out text tool — For deleting text when there is nothing to replace selection

Strikes through text in a red line.

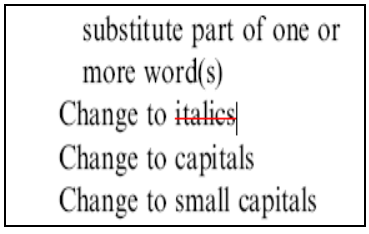

How to use it:

1. Select cursor from toolbar
2. Highlight word or sentence
3. Right click
4. Select Cross Out Text

Approved tool — For approving a proof and that no corrections at all are required.

How to use it:

1. Click on the Stamp Tool in the toolbar
2. Select the Approved rubber stamp from the 'standard business' selection
3. Click on the text where you want to rubber stamp to appear (usually first page)

Highlight tool — For highlighting selection that should be changed to bold or italic.

Highlights text in yellow and opens up a text box.

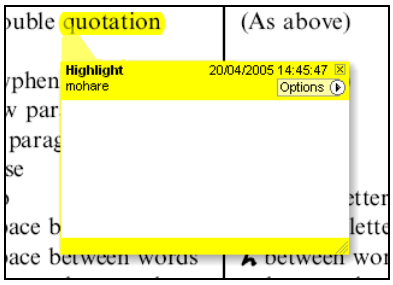

How to use it:

1. Select Highlighter Tool from the commenting toolbar
2. Highlight the desired text
3. Add a note detailing the required change

Attach File Tool — For inserting large amounts of text or replacement figures as a files.

Inserts symbol and speech bubble where a file has been inserted.

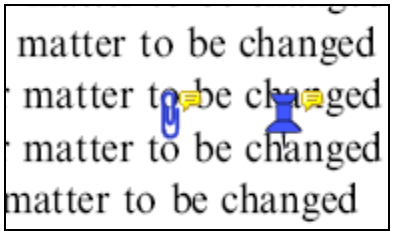

How to use it:

1. Click on paperclip icon in the commenting toolbar
2. Click where you want to insert the attachment
3. Select the saved file from your PC/network
4. Select appearance of icon (paperclip, graph, attachment or tag) and close

Pencil tool — For circling parts of figures or making freeform marks

Creates freeform shapes with a pencil tool. Particularly with graphics within the proof it may be useful to use the Drawing Markups toolbar. These tools allow you to draw circles, lines and comment on these marks.

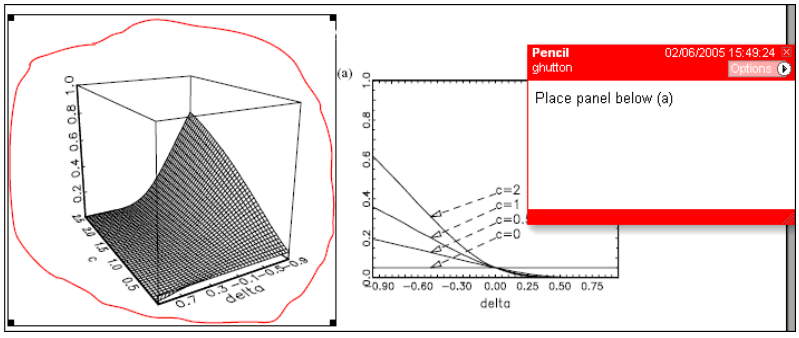

How to use it:

1. Select Tools > Drawing Markups > Pencil Tool
2. Draw with the cursor
3. Multiple pieces of pencil annotation can be grouped together
4. Once finished, move the cursor over the shape until an arrowhead appears and right click
5. Select Open Pop-Up Note and type in a details of required change
6. Click the X in the top right hand corner of the note box to close.

Help

For further information on how to annotate proofs click on the Help button to activate a list of instructions: